# Active Control of Bending Vibration in Magnetically Suspended Flexible Rotor

S. AKISHITA AND T. MORIMURA

## ABSTRACT

This paper describes an active control of bending vibration in a magnetically suspended flexible rotor containing a large disc at the center. The rotor is modelled as an elastic beam possessed of large rotary inertia effect by using Finite Element Method. Active control effect is expressed on the basis of modal cost analysis. The rotor without a large disc can be controlled by two magnetic forces together with almost colocated displacement sensors. On the contrary the rotor with the disc has definitely distictive mode shape at the second and the higher mode. In order to furnish with sufficient active control effect the tilt signal of the disc must be applied to the feed back cotrol system. This prediction by the analysis was verified in the measurement of the stationary rotor.

## 1 INTRODUCTION

We should overcome the spill-over problem for controling the bending vibration of the flexible rotor suspended by magnetic bearing, since the elastic vibration has infinite degree of freedom. Some designing methods for the active control of the vibration were proposed[1~6], assuming the colocation of the sensor and the magnetic reacting force. The elastic vibration in the flexible rotor was modelled conventionally as the bending vibration governed by the continuously distributed mass and bending stiffness. This modeling is adequate as far as the rotary inertia of the largest mass such as disc is small compared with translational inertia. But the effect of the rotary inertia should be considered for the flexible rotor with a large disc[7], because the effect affects the eigen mode and then the feasible control strategy should be taken correspondingly. The flexible rotor we are treating has a large disc in the center and is supported by the magnetic bearings at the upper and lower end as shown in Fig.2. The mathematical model is introduced for the elastic motion of the cross sectional center along the axis of

Sadao Akishita and Tomonori Morimura, Dept. of Mechanical Engineering, Ritsumeikan University, Kita-ku, Kyoto 603, Japan

the rotor, in which the dynamics of the rotation prevails. Finite Element Model (FEM) is introduced to the rotor for the analysis of the control system. Modal cost analysis[8)] is applied on the basis of FEM for finding the most effective control strategy. The location of the sensors for the feed back control is examined for the stationary rotor. The experiment is conducted to verify the analysis on the effect of the rotary inertia of the disc.

## 2 ANALYSIS

### 2.1 Mathematical Model†

A flexible rotor containing a large disc in the center is treated as an axi-symmetric beam in this paper. As shown in Fig.1, $z$-axis is defined along the axis of rotation with angular velocity $\Omega$,where $z$-axis coincides with the axis of symmetry in case of $\Omega = 0$ and $w = 0$. The elastic deflection of the rotor is described with the position of the cross sectional center $w(z) = (w_x(z), w_y(z))$ in the $O - x, y$ plane. Generally the slope of the deflection curve at the point $z$ can be written

$$\frac{\partial w(z,t)}{\partial z} = \psi(z,t) + \beta(z,t) \tag{1}$$

where $\psi(z,t)$ is angle of rotation due to bending and $\beta(z,t)$ is angle of distortion due to shear. But, $\beta(z,t)$ is neglected in this paper, for the effect of shear is small compared with that of bending. $\psi(z,t)$ has two components; $\psi(z) = (w_x'(z), w_y'(z))$, where prime means the derivative of $z$. The boundary condition at both ends of the rotor mean free of moments showing as

$$M_x = EI\psi_x' = 0 \quad or \quad w_x'' = 0 \quad at\ z = z_u \ and\ z_l \tag{2}$$

$$M_y = EI\psi_y' = 0 \quad or \quad w_y'' = 0 \quad at\ z = z_u \ and\ z_l \tag{3}$$

where $M_x$ and $M_y$ mean bending moment along $x$-axis and $y$-axis respectively, $EI(z)$ is bending stiffness of the cross sectional area, and $z_u$ and $z_l$ mean the $z$ positions of the upper end of the rotor and the lower end of the rotor respectively. The equations of elastic motion in the projection of the rotor to the $O - x, z$ plane are presented as

$$m(\ddot{w}_x - 2\Omega\dot{w}_y) = p_x \tag{4}$$

$$mk^2\ddot{\psi}_x - \frac{\partial}{\partial z}(EI\psi_x') + m\Omega k_z^2\dot{\psi}_y = 0 \tag{5}$$

where dot means the derivative of time, $k^2$ is the square of the radius of gyration around $x$ and $y$ axis, $k_z^2$ is the square of the radius of gyration around $z$ axis, and $p_x$ is the external shear force along $x$ axis. The similar equations in the projection to $O$-$y, z$ plane are presented as

$$m(\ddot{w}_y + 2\Omega\dot{w}_x) = p_y \tag{6}$$

† New FEM model of flexible rotor was published very recently by Gmur,T.C. and Rodigues,J.D.[9)]

$$mk^2\ddot{\psi}_y - \frac{\partial}{\partial z}(EI\psi_y^{'}) - m\Omega k_z^2\dot{\psi}_x = 0 \tag{7}$$

where $p_y$ is the external shear force along $y$ axis. The integral forms considering the boundary conditions are presented as

$$\int_{z_l}^{z_u} \left\{ m(\dot{w}_x^2 - 2\Omega w_x \dot{w}_y + k^2\dot{\psi}_x^2 + k_z^2\Omega\psi_x\dot{\psi}_y) + EI\psi_x^{'2} \right\} dz = \int_{z_l}^{z_u} p_x w_x dz \tag{8}$$

$$\int_{z_l}^{z_u} \left\{ m(\dot{w}_y^2 + 2\Omega w_y \dot{w}_x + k^2\dot{\psi}_y^2 - k_z^2\Omega\psi_y\dot{\psi}_x) + EI\psi_y^{'2} \right\} dz = \int_{z_l}^{z_u} p_y w_y dz \tag{9}$$

## 2.2 FEM Equations of Flexible Rotor

The elastic deflection of the rotor with a large disc is described with Finite Element Method in the paper. The elastic deflection variables are defined at $(n+1)$ node points of $n$ segments of the rotor with vector $q$,

$$q = [\ q_1^T, \cdots, q_{n+1}^T\ ]^T \tag{10}$$

$$q_i = [w_{xi}, l_0\psi_{xi}, l_0^2\psi_{xi}^{'}, w_{yi}, l_0\psi_{yi}, l_0^2\psi_{yi}^{'}], \quad (i = 1, \cdots, n+1)$$

where $l_0 = z_u - z_l$. Then FEM equation is described as follows,

$$M\ddot{q} + G\dot{q} + Kq = f \tag{11}$$

where $M$ is mass matrix and $K$ is stiffness matrix. $G$ is skew-symmetric matrix caused by Coriolis force and gyroscopic moment. $f$ is the generalized external force including the external shear force.

For a non-rotational rotor FEM equation is simplified as

$$M_1\ddot{q} + K_1 q = f_1 \tag{12}$$

where $M_1$ and $K_1$ are mass and stiffness matrix of a non-rotating rotor. The vector variable $q$ in Eq.(12) contains only half of components in Eq.(11), since the components along $x$ axis are common in those along $y$ axis for a non-rotational rotor. We are interested in the transfer function from the control force of magnetic bearing to the elastic deflection of rotor, which is governed by the eigen mode of FEM equation. As $G$ matrix in Eq.(11) is affected by the rotational speed $\Omega$, eigen mode characteristics of flexible rotor vary with $\Omega$. The bending vibration of flexible rotating shaft is clarified by solving Eq.(11) for each of the rotational speed. But what we are interested in is the large rotary inertia effect of the disc. The basic characteristics of the effec are retained in the behavior of stationary rotor. Therefore we focus our analysis on Eq.(12) in the study. $f_1$ in Eq.(12) is the generalized force vector composed of $3(n+1)$ components. For magnetic bearing the external forces exerted on the rotor are magnetic supporting forces represented by the force vector $u$ composed of $m$ descretized shear forces as shown by

$$u = [\ P_1, \cdots, P_m\ ]. \tag{13}$$

Then $f_1$ is expressed as follows with matrix $B$ that assigns $P_i$ to the corresponding node point.

$$f_1 = Bu, \qquad B : 3(n+1) \times m \tag{14}$$

## 3 ESTIMATION OF EFFECT OF VIBRATION CONTROL

Though the damping effect of the rotor structure is neglected in the above FEM equations, the damping effect term $D\dot{q}$ should be added to Eq.(12), for the rotor actually retains it even a little.

$$M_1\ddot{q} + D\dot{q} + K_1 q = Bu \tag{15}$$

where $D$ is damping matrix and is assumed to be related with $M_1$ and $K_1$ as $D = \alpha M_1 + \beta K_1$. The equation of the sensor signal is presented by the deflection vector $q$ and its time derivative,

$$y = Pq + R\dot{q} \tag{16}$$

where $P$ and $R$ matrices assign the sensor signals to the deflection and the vibrating velocity of the rotor at the sensor node points.

Modal cost analysis[8)] is applied for estimating the effect of the active control to bending vibration in the flexible rotor. So, the mode-decoupled form of Eq.(15) is introduced. The transfer matrix $\Phi$ composed of the eigen vectors of 1 to $k$-th order is correlated with matrices $M_1$ and $K_1$ as follows,

$$\Phi^T M_1 \Phi = I, \qquad \Phi^T K_1 \Phi = \Sigma^2, \qquad \Phi^T D \Phi = 2\zeta\Sigma \tag{17}$$

where $\Sigma$ and $\zeta$ are defined as

$$\begin{cases} \Sigma = diag.(\omega_1, \cdots, \omega_k), \qquad \zeta = diag.(\zeta_1, \cdots, \zeta_k) \\ 2\zeta\Sigma = diag.(2\zeta_1\omega_1, \cdots, 2\zeta_k\omega_k) \end{cases} \tag{18}$$

The vector $q$ is transfered to $x$ by using $\Phi$, $\Sigma$ and $\zeta$,

$$\begin{bmatrix} q \\ \dot{q} \end{bmatrix} = \begin{bmatrix} \Phi & \Phi \\ \Phi\Lambda_c & \Phi\bar{\Lambda}_c \end{bmatrix} x \tag{19}$$

where $\Lambda_c$ and $\bar{\Lambda}_c$ are defined as

$$\Lambda_c = -\zeta\Sigma + j\Sigma(1-\zeta^2)^{\frac{1}{2}}, \qquad \bar{\Lambda}_c = -\zeta\Sigma - j\Sigma(1-\zeta^2)^{\frac{1}{2}} \tag{20}$$

where $j$ means the imaginary unit. Applying column vector $x$ of $k$-th order, Eqs.(15) and (16) are transfered as follows

$$\dot{x} = \begin{bmatrix} \Lambda_c & O \\ O & \bar{\Lambda}_c \end{bmatrix} x + \begin{bmatrix} -I \\ I \end{bmatrix} (\bar{\Lambda}_c - \Lambda_c)^{-1} \Phi^T B u \tag{21}$$

$$y = [P\Phi + R\Phi\Lambda_c, P\Phi + R\Phi\bar{\Lambda}_c] x \tag{22}$$

where $I$ is the identity matrix of $k$-th order. Cost function $V$ of output signal $y$ is introduced as follows

$$V = \int_0^{\infty} y^* Q y dt \tag{23}$$

where asterisk means to evaluate $y$ by the transposed conjugate of the original complex vector, and $Q$ is the weighting matrix assumed as semi- positive definite. Modal cost is defined as modal component of cost function $V$ in the case where the system is excited by impulse input. We evaluate input $u$ by covariance matrix $U$, $i$-th diagonal component of which is represented as follows by the impulse of strength $s_i$

$$U = diag.(\cdots, s_i^2, \cdots)$$

When we define $i$-th column of matrix $P\Phi + R\Phi\Lambda_c$ as $c_i$, cost function $V$ is rewritten by

$$V = \sum_{i=1}^{k} \sum_{j=1}^{k} X_{ij} c_j^* Q c_j \tag{24}$$

where asterisk means to evaluate $c_j$ by the transposed conjugate of the original complex vector again. $X_{ij}$ $(1 \leq i, j \leq k)$ is the component of $i$-th row and $j$-th column of the covariance matrix of $x$, which are derived by solving the equation of the covariance matrix. We assumed above that the damping effect was very small, then the following approximation is valid,

$$\zeta_i \ll \frac{|\omega_i - \omega_j|}{2\omega_i}, \qquad {}^{\forall} j \neq i \tag{25}$$

Henceforth the following relation is justified.

$$X_{ii} \gg |X_{ij}|, \qquad {}^{\forall} i \neq j \tag{26}$$

We should add that $X_{ii}$ is equal to $X_{i+k,i+k}$. Finally cost function $V$ is rewritten mode by mode with the equation

$$V = \sum_{i=1}^{k} = \sum_{i=1}^{k} \frac{b_i^* U b_i c_i^* Q c_i}{\zeta_i \omega_i} \tag{27}$$

where $b_i^*$ is defined as the $i$-th row vector of $(\bar{\Lambda}_c - \Lambda_c)^{-1} \Phi^T B$, and $b_i^*$ is defined as its transposed conjugate.

## 4 RESULT OF CALCULATION AND EXPERIMENT

### 4.1 Object of Investigation

The schematic configuration of the magnetically suspended rotor we are investigating is shown in Fig.2. The rotor cotaining circular disc of $150^{\phi} \times 100mm$ in the center are supported vertically by magnetic bearings at the upper and lower ends. The configuration of the disc is varied to such shape as illustrated with dotted line. The diameter of the smaller disc is $42mm$ and the moment of inertia of the disc is decreased drastically. The rotor is actively controlled in the radial four axis motion by the upper and lower radial magnetic bearings, and in the vertical motion by the axial magnetic bearings. The radial displacement sensors locate at shifted axial position from the corresponding magnetic reaction point. So, the colocation condition between the actuators and sensors is not strictly realized.

### 4.2 The Result of Calculation

The eigen frequencies and the corresponding eigen mode shapes of bending motion are calculated on the basis of FEM mentioned at section 2.2. The rotor is divided into 24 blocks both for the case with the large disc and for the case without that. Figure 3 (a) and (b) illustrate the eigen frequencies and the mode shapes from first to fourth mode for both cases. The eigen frequency differs largely from each other. The mode shape is similar in both at first and second mode, where we should note that the displacement at the disc position (the symbol $\bigtriangledown$ is marked in the figure) is definitely zero in the case with the disc while it is finite in the case without the disc. Actually the mode shape differs largely in both at third and fourth mode, then the effect of the rotary inertia of the disc is remarkable for the case with the disc. We are calculating the modal cost mentioned at section 3 about these modes. The control inputs are the radial forces by the magnetic bearings and the outputs are fed by the corresponding displacement sensors in the calculation. $\zeta_i = 0.003$, $s_i = 1$ $(i = 1, \cdots, k)$ and $Q = I$ are assumed there. Figure 4 shows the modal cost for the case without the disc. Abscissa means the frequency of the mode in the figure. The value of the cost is normalized by the largest cost hereafter. The second mode has the largest cost and the cost decreases generally with the mode number. Figure 5 shows the modal cost for the case with the disc. We can find that the second mode has definitely small cost compared with the first and the third mode on the contrary. This means that the active control by the magnetic bearings cannot govern the sensor output signal of the second mode, because the slope of the deflection curve of the flexible rotor prevails at the second mode shape but the deflection itself does not prevail as mentioned above. This tendency exhibits also in the transfer function from the control force by the magnetic bearing to the corresponding displacement at the closest sensor position. Figure 6 shows the transfer function of the rotor without the disc, and Fig.7 shows the transfer function of the rotor with the disc. The gain at the second mode peak decreases considerably for the rotor with the disc, while the gain at the second mode peak has the same order magnitude as the other mode peaks for the rotor without the disc. In order to improve the controllability to the second mode the slope signal of the deflection should be utilized. Figure 8 shows the improved modal cost for the case with the disc, where the tilt signal of the disc is fed to the output. The modal cost of the second mode increases remarkably (see $\bigcirc$ symbol in Fig.8) compared with the cost in Fig.5.

### 4.3 The Result of Experiment

As mentioned above main objective of the paper is to clarify the effect of the large rotary inertia of the disc for the stationary rotor. The experiment is confined to the stationary rotor. The accuracy of the calculation is verified by the measurement of the spectrum of the free bending vibration in the rotor without the disc suspended by the magnetic bearings as shown in Fig.9. The first to third mode frequencies coincide almost with that of calculation ($82Hz, 293Hz, 578Hz$ respectively) in the figure as shown by the number (1) to (3). PID controller is applied for the magnetic suspension systems, assuming the approximated colocation condition of the sensors and the actuators. The magnetic suspension experiment was conducted for the rotor with the disc. Figure 10 (a) shows the spectrum of the free bending deflection in the rotor with the disc suspended by the magnetic bearings, where only the deflection signal of the rotor was utilized in the feed back control of the suspension. The marked peak is found at $135Hz$ that is nearly equal to the calculated second mode frequency $137Hz$. When the disc tilt signal was fed to the suspension control force, the second peak disappeared in the spectrum as shown in Fig.12 (b). The prediction from the modal cost analysis was proved by the measurement.

## 5 CONCLUDING REMARKS

FEM analysis was conducted on the active control of the bending vibration in the flexible rotor with the large disc. The effect of the rotary inertia of the large disc in the center of the rotor was predicted at the second and the higher eigen mode. The modal cost analysis predicted that the feed back control utilizing the bending deflection signal could not govern the second mode vibration, and that the bending vibration of the second mode could be improved by utilizing the tilt signal of the disc to the control. The analysis was verified at the second mode vibration by the measurement.

Reference

1. Salm,J.R., "Active Electromagnetic Suspension of an Elastic Rotor; Modelling, Control, and Experimental Results " , ASME Journal of Vibration and Acoustics, Vol.110, pp.493, 1988.

2. Akishita,S. and Hayashi,K., "Vibration Control on Magnetically Suspended Flexible Beam ", ASME Computers in Engineering, Book No.G0515A- 1990.

3. Humphris,R.R. et al., "Effect of Control Algorithms on Magnetic Journal Bearing Properties ", ASME Journal of Engineering for Gas Turbines and Power, Vol.108, 1986, pp.624–632.

4. Burrows,C.R. et al. "Design and Application of a Magnetic Bearing for Vibration Control and Stabilization of a Flexible Rotor ", Proc. First International Symposium on Magnetic Bearings, ETH Zurich, 1988, pp.159–168.

5. Anton,A. and Ulbrich,H., "Active Control of Vibration in the Case of Asymmetrical High-Speed Rotors by Using Magnetic Bearings ", ASME Journal of Vibration and Acoustics, 1985, 85-DET-28.

6. Okada,Y. et al., "Cross-Feedback Stabilization of the Digitally Controlled Magnetic Bearing ", ASME Journal of Vibration and Acoustics,Vol.114, 1992, pp.54–59.

7. Timoshenko,S., Young,D.H. and Weaver, W.Jr., "Vibration Problem in Engineering ", 4th ED., John Wiley & Sons 1974.

8. Skelton, R.E., "Dynamic System Cotrol ", John Wiley & Sons, 1988.

9. Gmur,T.C. and Rodrigues,J.D., "Shaft Finite Elements for Rotor Dynamics Analysis ", ASME Journal of Vibration and Acoustics, Vol.113, 1991, pp.482–493.

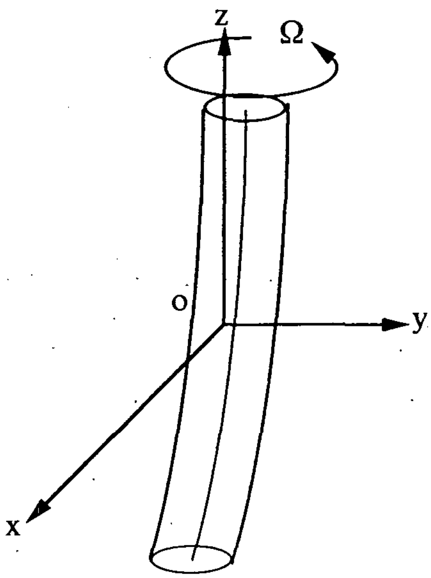


Fig.1 Definition of coordinate

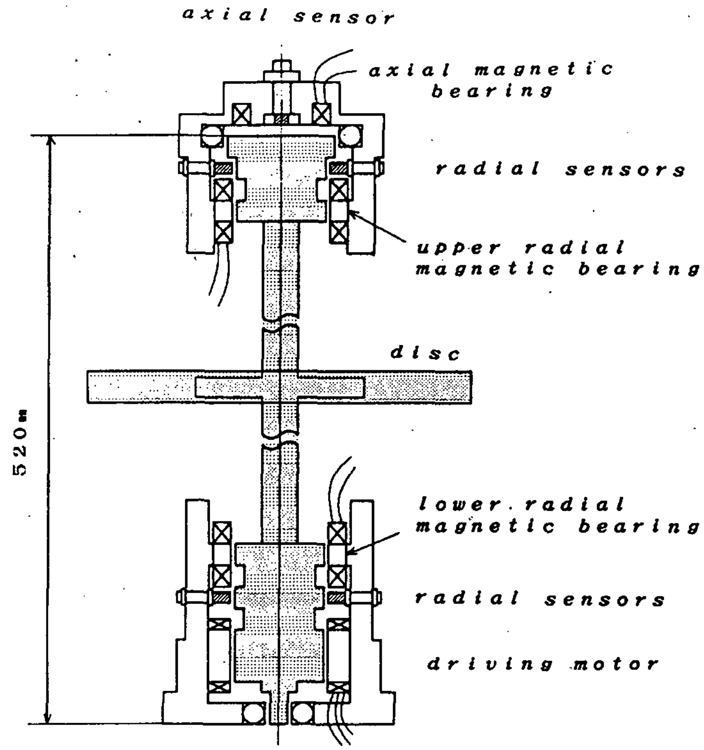


Fig.2 Magnetic bearing and suspended flexible rotor

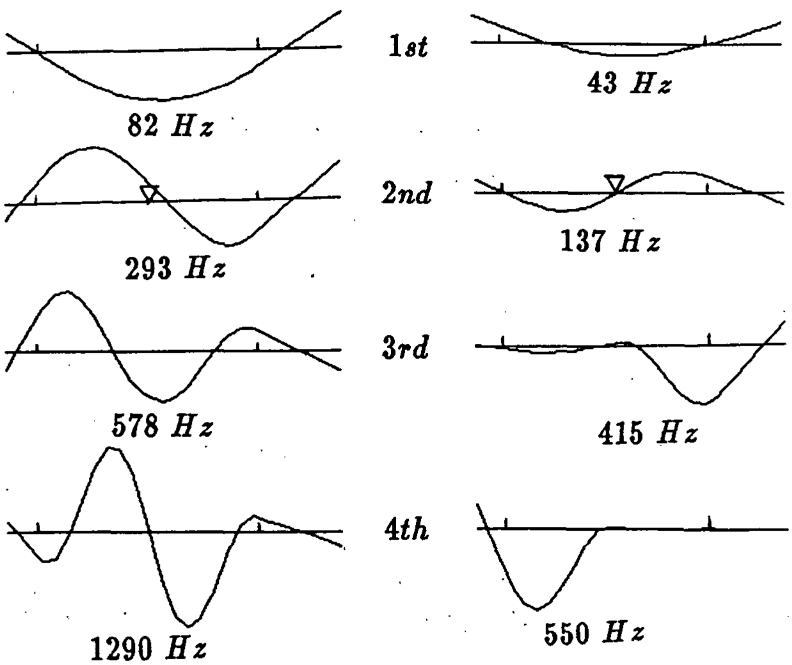


(a)without the disc (b) with the disc

Fig.3 Mode shape of bending vibration

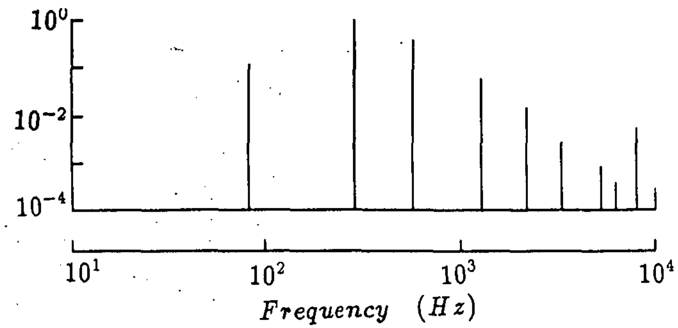


Fig.4 Modal cost without the disc

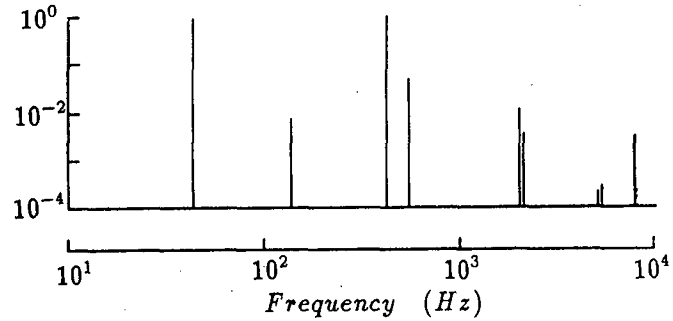


Fig.5 Modal cost with the disc

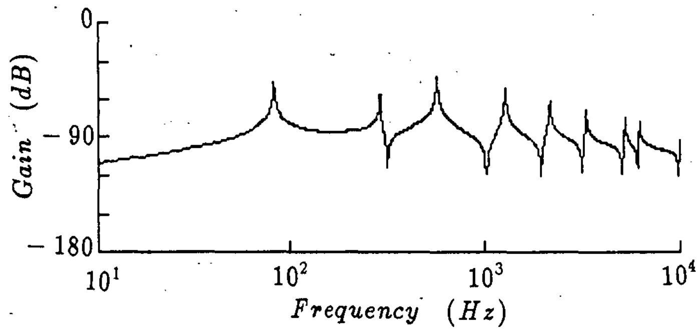


Fig.6 Transfer function without the disc

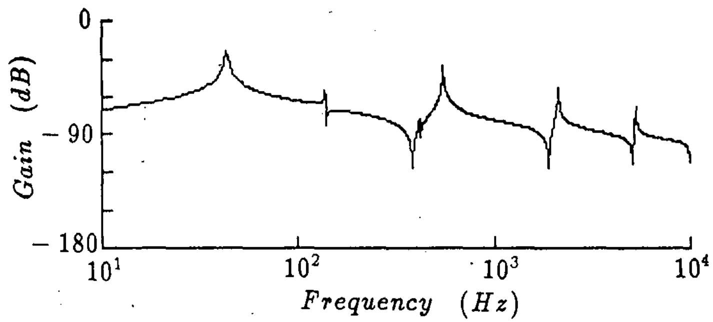


Fig.7 Transfer function with the disc

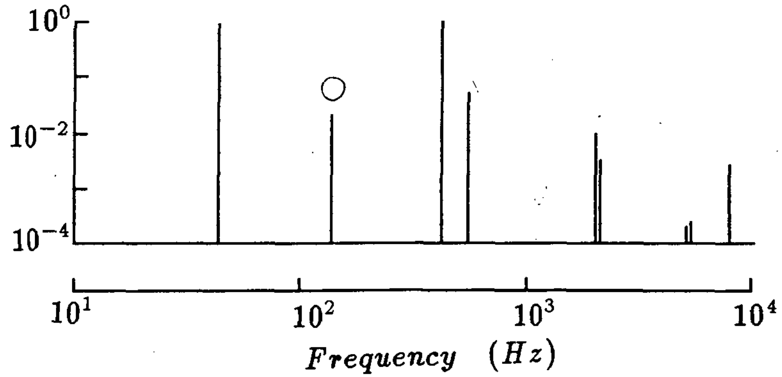


Fig.8 Modal cost for the improved rotor with the disc

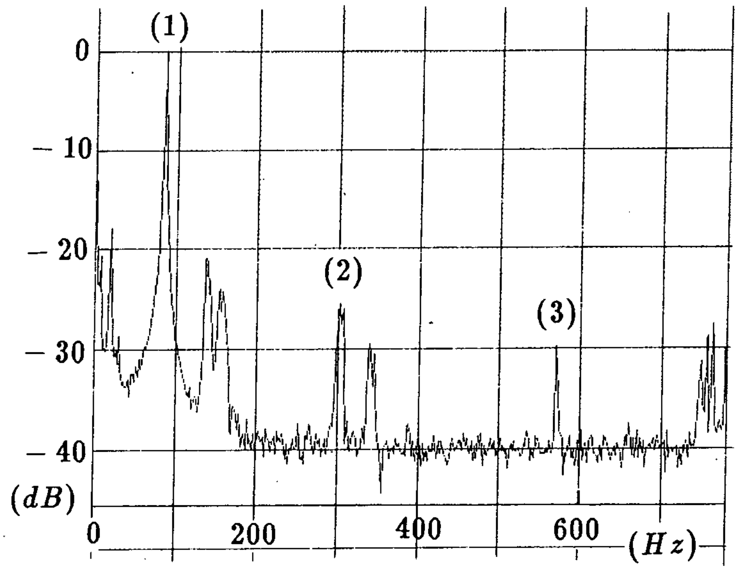

Fig.9 Spectrum of free bending vibration in the rotor without the disc

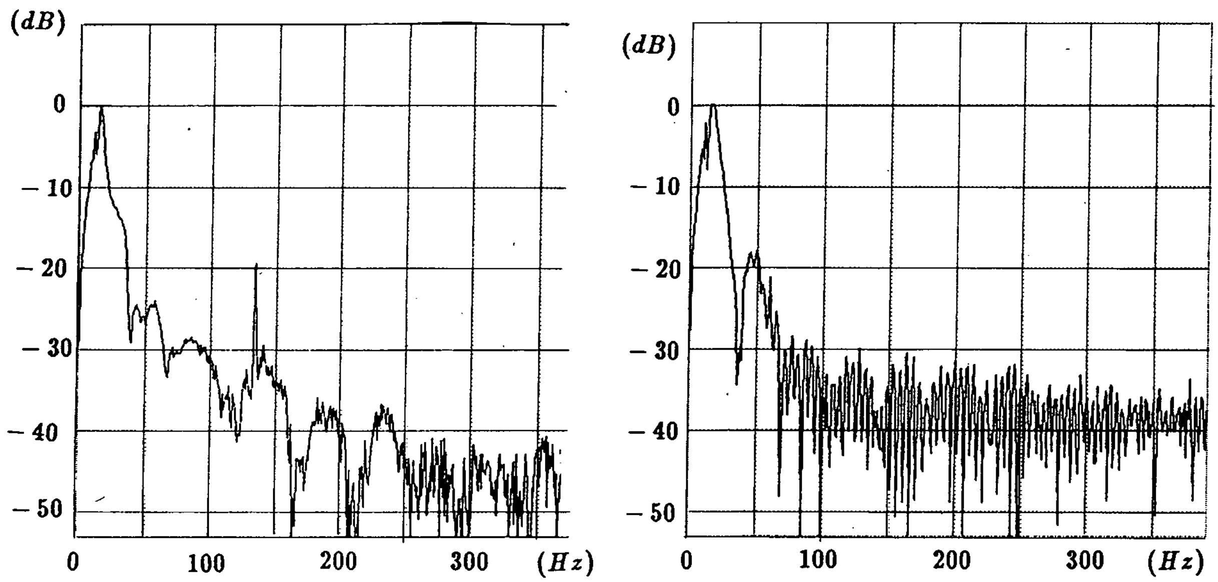

(a) without the tilt signal

(b) with the tilt signal

Fig.10 Spectrum of free bending vibration in the rotor with the disc